Colloid Polym Sci 273:496–504 (1995)
© Steinkopff Verlag 1995

ORIGINAL CONTRIBUTION

O. Karlsson
H. Hassander
B. Wesslén

Particle size measurements of heterogeneous film-forming latexes

Received: 13 April 1994
Accepted: 9 November 1994

O. Karlsson · H. Hassander
B. Wesslén (✉)
Lund Institute of Technology
Chemical Center
Department of Chemical Engineering II
P.O. Box 124
221 00 Lund, Sweden

Abstract Two-phase latex particles consisting of mainly polystyrene (PS) and polyisoprene (PI) in ratios varying from 70:30 to 20:80 were prepared using different polymerization techniques. Methacrylic acid (MAA) was used in small amounts as a comonomer. The latexes had narrow size distributions, and showed different particle morphologies depending on the monomer composition and the polymerization conditions used. In most cases the latexes were film-forming at room temperature. Particle size distributions and average particle sizes of the latexes have been determined using different particle sizing methods.

Size determination by TEM was performed after staining with osmium tetroxide (OsO_4) or uranyl acetate (UAc). The staining methods showed no significant differences in particle size averages and particle size distributions when the ratio between the PI and PS phases did not exceed 50:50. At higher phase ratios OsO_4 staining was preferred. The glass transition temperature of the PI phase increased after OsO_4 staining, which prevented deformation of the latex particles. Particle morphologies for the heterogeneous latex particles were also determined after OsO_4 staining.

Particle sizes measured by TEM were generally smaller than the corresponding sizes measured by quasielastic light scattering (QELS). The difference in the measured diameters increased with increasing PI and PMAA content in the latex particles. The larger sizes observed by QELS are results of the presence of an immobilized water layer surrounding the particles in the aqueous environment, water absorption and swelling due to the presence of carboxylic acid groups, and adsorption of soluble carboxylated polymers forming a hydrophilic corona around the particles. By TEM the hard sphere diameters of dehydrated particles are measured.

Key words Heterogeneous latexes – particle size – transmission electron microscopy (TEM) – staining – quasielastic light scattering (QELS)

Introduction

The particle size distribution of a dispersion influences many important properties, for example, viscosity, turbidity and sedimentation velocity, and may be used as a quality assessment for products such as latex paints or fillers for plastics. In paint applications the size of the latex particles influences film formation and gloss. Also, measurements of particle size averages and size distributions for polymer latexes are important for ascertaining reproducibility in emulsion polymerization processes.

Film-forming heterogeneous latex particles have interesting properties for coating applications. The latex particles are prepared by a seeded emulsion polymerization, which is carried out in two or more steps. In this process the control of new particle formation is important. Particle size analysis after each one of the consecutive steps in the process may be used to detect formation of new particles, provided the analytical methods give the correct information on the particle size distribution. In the present study particle size distributions for heterogeneous carboxylated film-forming latexes have been examined, and techniques for measuring particle sizes and size distributions were compared. Because of the film-forming properties of the latexes different measuring methods may give different results, and the aims of the investigation were to analyze the differences between some commonly used methods. The latex samples were analyzed by transmission electron microscopy (TEM) using various staining techniques, and the average diameters calculated were compared to particle diameters obtained by quasielastic light scattering (QELS).

Experimental

Preparation of latexes

Styrene (Merck, *pro analysi*), isoprene (Merck, *pro analysi*), and methacrylic acid (Merck, *pro analysi*) were purified from inhibitors by passing the monomers through a column filled with aluminum oxide (Merck, active base). The purified monomers were kept at 8 °C before use. All other chemicals were of analytical grade and used as supplied. Distilled and deionized water was used.

Latexes were prepared using a two-step seeded emulsion polymerization process run at 80 °C with potassium persulfate as the initiator and sodium dodecyl sulphate (SDS) as the emulsifier. The seed latex was prepared through a batch polymerization in a 2000 ml reactor. The seed consisted of poly-(St-*co*-MAA) containing varying amounts of MAA. The reactor containing the monomers, surfactant, and water was degassed and purged with nitrogen repeatedly before the temperature was raised and the initiator added. The compositions of the seed latexes are given in Table 1.

The second polymerization step was carried out in a 200 ml calorimetric reactor which has been described in detail by Nilsson et al. [1]. The polymerization was either performed as a batch process or as a semi-batch process with continuous addition of the second step monomers. In the batch experiments the reactor containing the seed latex and the second step monomers, i.e., isoprene, styrene, and MAA, was repeatedly degassed and purged with nitrogen at room temperature before the polymerization was started by increasing the temperature to 80 °C. Details on all polymerizations are given elsewhere [2].

Table 1 Compositions of seed latexes. Diameters reported are number averages, $\bar{D}_n$, obtained by TEM measurements with a mean standard deviation of 8 nm.

Seed	Composition (%)		Particle size (nm)	T_g (°C)
	Styrene	Methacrylic acid		
A	98	2	76	105
B	80	20	55	173
C	98	2	72	109
D	100	0	93	105

In the semi-batch experiments the second step monomers were degassed and purged with nitrogen before use. The monomers were either added continuously or, in some polymerizations, isoprene and styrene were added continuously while MAA was added at the end of the polymerization. The ratios between the second phase polymers and the seed varied in the range 80:20 to 30:70. The latex compositions are given in Table 2. The reactions were monitored by measuring the heat of polymerization.

DSC

Latexes were dried at room temperature for 48 h and the resulting films were analyzed by means of a Mettler DSC 30 equipped with a low temperature cell. The samples were first heated at 15 °C/min to 130 °C. After 5 min at 130 °C the samples were cooled down to −150 °C at a rate of 15 °C/min, and finally reheated to 250 °C at a scanning rate of 10 °C/min. The last run was used for determination of T_g.

Osmium tetroxide (OsO_4) stained films were also investigated by DSC. The OsO_4 staining was done in vapor phase for 1 h [3]. The osmium stained samples were first heated to 130 °C at a rate of 20 °C/min. After 3 min at 130 °C the samples were cooled down to −150 °C (20 °C/min), and reheated to 170 °C at a rate of 10 °C/min. The last run were used for determination of T_g.

Electron microscopy

Micrographs of the latex particles were obtained using a JEOL 100 U transmission electron microscope. The latexes were stained with osmium tetroxide (OsO_4) and uranyl acetate (UAc), respectively.

Osmium staining: Osmium tetroxide was allowed to react with residual double bonds in the polyisoprene (PI) phase

Table 2 Compositions and properties of heterogeneous styrene-isoprene latexes.

Latex	Composition step 2						Particle size[3] (nm)	T_g (°C)[4]	
	Seed	Phase ratio seed:step 2[1]	Method[2]	Styrene (%)	Isoprene (%)	Methacrylic acid (%)		Soft phase	Hard phase
1	A	50:50	B A1 A2	0	92	8	96	−42	104
2	A	50:50	B A1 A2	29	67	4	99	−25	97
3	A	47:53	B A1 A2	40	56	4	101	−13	99
4	A	47:53	B A1 A2	58	37	4	94	26	99
5	A	47:53	B A1 A2	0	88	12	92	−39	104
6	A	28:72	B A1	0	100	0	109	−59	106
7	A	28:72	B A1 A2	0	96	4	112	−50	105
8	A	28:72	B A1 A2	0	92	8	119	−47	102
9	A	28:72	B A1 A2	4	67	29	119	−23	104
10	A	47:53	B A1 A2	10	64	26	93	25	100
11	A	47:53	B A1	0	100	0	98	−58	107
12	B	67:33	B A1	0	100	0	59		
13	C	54:46	SB A1	0	100	0	94	−61	110
14	D	48:52	B	0	100	0	108	−66	104
15	D	19:81	B	0	100	0	163	−59	106
16	D	48:52	B A2	0	90	10	120	−45	104
17	D	19:81	B A2	0	90	10	152	−30	102
18	D	45:55	SB	0	100	0	125	−59	101
19	D	20:80	SB	0	100	0	162	−49	87
20	C	21:79	SB A1	0	100	0	129	−58	
21	C	50:50	SB A1 A2*	0	83	17	88	−62	108
22	C	39:61	SB A1 A2**	0	93	7	98	−56	105
23	C	43:57	SB A1 A2*	0	92	8	98	−58	105
24	D	45:55	SB A2*	0	91	9	126	−54	99
25	A	50:50	B A1	0	100	0	95	−56	103
26	A	50:50	B A1 A2	0	96	4	91	−51	103

[1] Phase ratios are based on weight.

[2] Polymerization method denotation:
B batch polymerization
SB semi batch polymerization
A1 acid charged in seed
A2 acid batch charged in step 2
A2* acid continuously added in step 2
A2** acid added at the end of step 2

[3] Diameters reported are number averages, $\bar{D}_n$, obtained by TEM measurements using OsO_4-staining with a mean standard deviation of 6 nm.

[4] Obtained by DSC.

of the latex particles. Generally, OsO_4 is introduced in vapor phase according to Kato [3]. The latex is diluted and a drop placed on a formvar-coated microscope grid and put in a sealed glass container together with a vial containing a 1 wt% aqueous OsO_4 solution. In the present case the latex particles will deform and form film if the latex has dried before the staining reaction is complete.

In order to avoid distortion of the latex particles the staining was carried out in the liquid phase. The latex was diluted to 0.1 wt %, and an equal volume of a 2 wt % OsO_4 solution was added. The sample was allowed to stand for 50–60 min at room temperature and a drop was then placed on a formvar-coated microscope grid, and the water allowed to evaporate. In the TEM micrographs the PI-containing phase appeared as dark domains and the seed phase as bright domains.

Uranyl acetate staining: Negative staining with UAc was performed for latexes no. 1, 2, 3, 4, 6, 7, 8, 14, 15, 17, 21, and 26 as described by Mahl [4]. The latexes were diluted to approximately 2 wt % and an equal volume of a 0.5 wt % UAc solution was added. The mixture was allowed to stand for 1 h, and a drop of the solution was then placed on a formvar grid. The sample was dried for 1 h at room temperature. With this staining method the PI-containing phase appeared as bright domains and the seed phase as dark domains.

Calibration grids were used for determining the actual magnification [5]. The diameters of individual particles were measured from the TEM micrographs. For each particle two orthogonal diameters were determined in order to minimize random errors in the measuring process [5]. For most latexes over 1000 diameters were measured for each sample in order to ensure precision in the measurements. The data were further processed for evaluation of particle size distributions and particle diameter averages.

Quasielastic light scattering

QELS measurements were performed using a Coulter Model N4MD particle sizer, which uses a version of the computer program CONTIN to perform the inversion of the composite autocorrelation function [6, 7].

Prior to the QELS measurements the latexes were diluted with doubly distilled, deionized, and doubly filtered (Millipore, 100 nm) water in order to minimize the influence of dust particles. The diluted samples were buffered at pH 7.0 with a phosphate buffer having a ionic strength of 3.0×10^{-3} mole/L, SDS was added to a concentration of 6.9×10^{-3} mole/L, and the samples were finally sonicated for dispersion of any aggregates. The measurements were performed at 20 °C at a scattering angle of 90°. Generally, the results reported are averages of 10 runs having a dust factor of 0%.

Results and discussion

Preparation of heterogeneous latex particles

Heterogeneous latex particles were prepared by a seeded two-step emulsion polymerization. Polystyrene (PS) particles containing different amounts of MAA were prepared in the first step, and then used as seeds for the second step in which isoprene, styrene, and MAA were polymerized in a batch or semi-batch process. In the semi-batch process the MAA was either added continuously together with the other monomers, or at the end of the polymerization. Data for the latexes prepared are collected in Table 2.

Particle size analyses, carried out as discussed below, showed that the latexes had narrow, unimodal particle size distributions. Depending on the monomer composition and the polymerization conditions used, different particle morphologies were obtained. The major factor influencing the particle morphology was found to be the hydrophilic properties of the two phases, and by using different methods for the addition of the MAA the hydrophilicity of the second phase polymer could be controlled. Different morphologies were observed, for example, "sandwich-like" and "halfmoon-like" according to Cho and Lee [8], and "inverted core-shell" as reported by Lee and Ishikawa [9]. A detailed analysis of the factors influencing the morphology of the styrene-isoprene latexes will be reported elsewhere [2].

Films prepared from the latexes were all analyzed by DSC, and the results presented in Table 2 clearly show that the polymers display two different glass transitions, i.e., two separate polymer phases were present. The glass transition found at about 100 °C can be ascribed to the PS seed. The second glass transition, which is attributed to the second polymer phase, varies from −66 °C to +25 °C, depending on the composition. The properties of the composite latex particles depended on their morphology, but in most cases they were film-forming at room temperature.

Particle size determination by TEM

Because of the isoprene-rich second, outer phase the composite latex particles were generally quite soft at the temperatures used for TEM analysis and for sample preparation, and problems with deformation of the particles and film formation were encountered on preparation of the TEM samples. These problems may be overcome by staining and hardening of the latex particles before TEM analysis, or by the use of a cryo stage [10], or by combinations of different methods [11–13]. Staining techniques include positive staining, i.e., reaction of residual double bonds in the latex particles with osmium [3] or with bromine [14], and negative staining with UAc [4] or phosphotungstic acid [15].

In the present study, we have investigated one negative and one positive staining method. Negative staining was done with UAc, which leaves shadows of the particles on the microscope grid even if the particles have decomposed or become deformed in the electron beam. UAc [16] as well as phosphotungstic acid [15] may also act as positive staining agents by reacting with functional groups in the particle surface, e.g., hydroxylic and carboxylic groups. There is probably little diffusion of UAc into the particles.

OsO_4 was used for positive staining. The reagent diffuses very slowly into the particles and reacts chemically with residual double bonds present in the PI-containing phase of the composite particles. Because of the reaction with OsO_4, T_g of the polymer increases. This effect is illustrated in Fig. 1 which shows that the glass transition of a latex stained with OsO_4 increases by approximately 30 °C, as compared to the untreated latex. The increase in T_g depends on the duration of the OsO_4 treatment. The osmium treated particles become more rigid and do not easily deform in the electron beam.

Twelve latexes were examined after staining with UAc (see Experimental part). If these latexes were considered as one homogeneous group, different particle size averages were obtained with OsO_4 and UAc staining, respectively, as reported in Table 3a. The deviations could be attributed to a sub-group of latexes consisting of no. 6, 7, 8, 15 and 17,

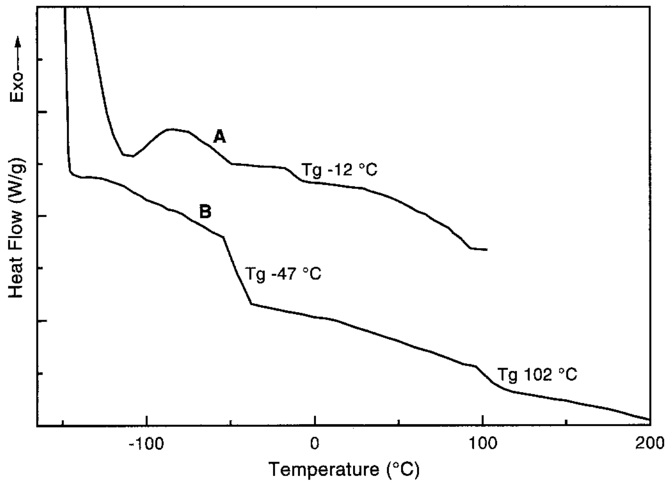

Fig. 1 DSC traces for an OsO_4 stained latex (A) and the original latex (B)

which had hemisphere morphologies and a PI:PS phase ratio exceeding 70:30. When this sub-group was excluded the comparison gave statistically similar averages (Table 3b). The average values agreed within a 95% confidence interval and the standard deviation for the comparison of the two methods decreased significantly.

A comparison done with the excluded sub-group of latexes showed that the two staining methods gave significantly different average particle sizes (Table 3c). The latexes in this group are film-forming below room temperature, and true particle diameters are difficult to obtain by UAc staining. As soon as the water evaporates from the latex the soft PI phase deforms and starts to form film, and the true particle diameters will consequently not be obtained.

In Fig. 2 the effects of the different staining techniques are shown for latex samples no. 7 and 15. The particles in both these samples have a so-called "halfmoon" or hemisphere morphology. In latex no. 7 the more hydrophilic poly-(I-*co*-MAA) phase is trying to engulf the PS seed phase, while in latex no. 15 the PS seed phase forms a hemisphere around the more hydrophobic homo-PI phase. Both latexes are film-forming at room temperature, and the mechanical properties of the films are similar to PI. When the latexes were stained with OsO_4 the particles retained their spherical shapes, as can be seen in Figs. 2A and 2B. The particle morphology is shown by the TEM micrographs; the lighter areas in the particles being the PS phase and the darker areas the OsO_4-stained PI phase. Particle sizes can easily be measured from this type of micrograph. Figures 2C and 2D show the same latexes after staining with UAc. As evident from the micrographs, the latex particles have deformed and started to form film before the TEM analysis. The soft PI phase has spread on the grid, which increases the apparent particle diameters. UAc does not penetrate into the particles but collects as a dark boundary surrounding the PI phase (Figs. 2C and 2D). The data for latex no. 15 in Table 4 show that UAc staining gave approximately 30% larger average diameter and a much wider size distribution than OsO_4 staining. The PS hemispheres present in the latex particles were not affected by the film formation process or by the electron beam in the microscope, as indicated in Figs. 2C and 2D. For latex no. 15 (Fig. 2C) the hemispheres are faintly visible in the center of the dark circular boundary of UAc. The hemisphere sizes were measured

Table 3 The statistics from comparison of different particle size measurement methods with a 95% confidence interval.

	a $\bar{D}_{n,\mathrm{UAc}} - \bar{D}_{n,\mathrm{OsO_4}}$	b $\bar{D}_{n,\mathrm{UAc}} - \bar{D}_{n,\mathrm{OsO_4}}$	c $\bar{D}_{n,\mathrm{UAc}} - \bar{D}_{n,\mathrm{OsO_4}}$	d $\bar{D}_{\mathrm{LS,OsO_4}} - \bar{D}_{\mathrm{I,QELS}}$	e $\Delta D_{\mathrm{Observed}} - \Delta D_{\mathrm{Predicted}}$
$\bar{d}$	14.5	3.5	30.0	15.4	0.0
N	12	7	5	24	24
S_d	16.8	6.8	13.8	10.9	4.7
t_0	3.0	1.35	4.85	6.95	4×10^{-6}
$t_{0.05/2,n-1}$	2.20	2.45	2.78	2.07	2.07
Reject H_0	Yes	No	Yes	Yes	No

a) Comparison of UAc staining and OsO_4 staining for all investigated latexes.
b) Comparison of staining with UAc and OsO_4 for latexes nos. 1, 2, 3, 4, 14, 21 and 26. Step 2: seed phase ratio 50:50 or less.
c) Comparison of staining with UAc and OsO_4 for latexes nos. 6, 7, 8, 15 and 17. Step 2: seed phase ratio 70:30.
d) Comparison of the intensity average, $\bar{D}_I$ obtained from QELS and the light scattering average, $\bar{D}_{LS}$ obtained from TEM after staining with OsO_4.
e) Comparison of the observed ΔD, and the predicted ΔD obtained from the response surface equation.

Symbols used: $\bar{d}$ = sample mean of the computed paired differences, N = number of samples, S_d = sample standard deviation of the differences, t_0 = test statistic used for comparing different methods, $t_{\alpha/2,n-1}$ = t distribution with $1 - \alpha$ confidence limit and $n - 1$ degrees of freedom, H_0 = null hypothesis.

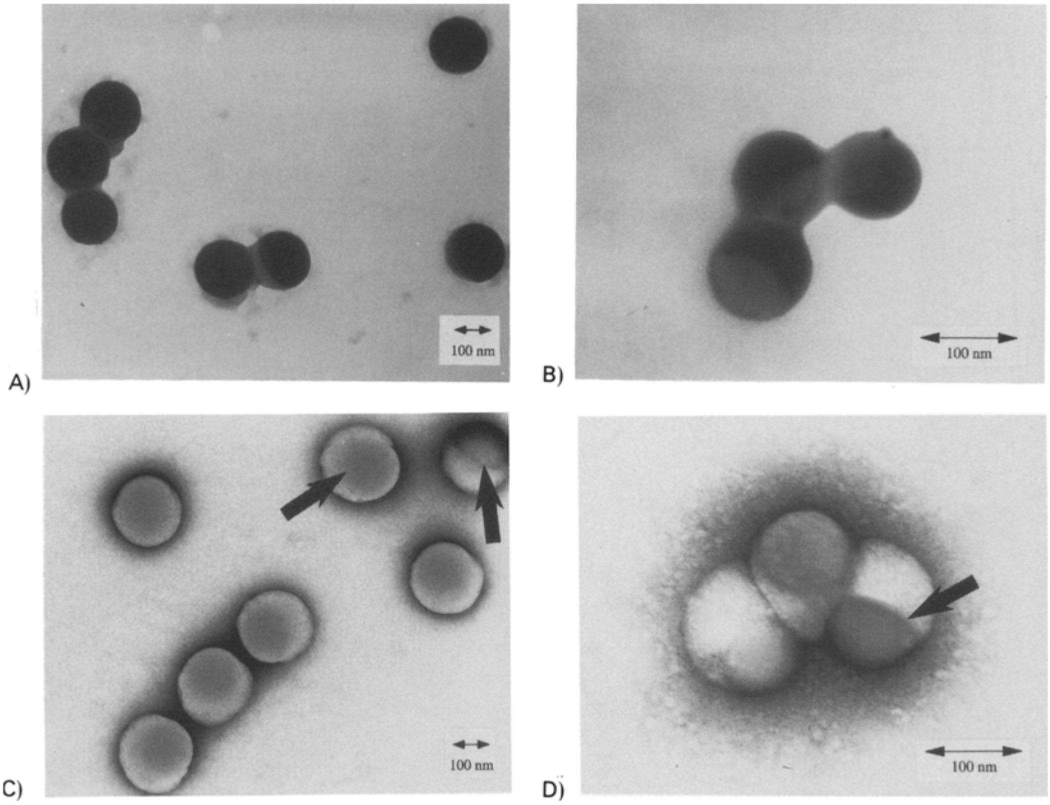

Fig. 2 A) TEM micrograph of OsO_4-stained latex no. 15. B) TEM micrograph of OsO_4-stained latex no. 7. C) TEM micrograph of UAc-stained latex no. 15. D) TEM micrograph of UAc-stained latex no. 7. In C) and D) the spherical shapes of the particles are not preserved. The PS hemispheres, indicated by arrows, are preserved and are not affected by the film formation process

Table 4 Comparison of different staining methods used in TEM for latexes nos. 14 and 15. For latex no. 15 the PS hemisphere diameters obtained with different staining methods are given.

	UAc				OsO_4			
Latex	$\bar{D}_n$ (nm)	σ (nm)	N	PDI = $\bar{D}_n/\bar{D}_w$	$\bar{D}_n$ (nm)	σ (nm)	N	PDI = $\bar{D}_n/\bar{D}_w$
14	115	7.3	1050	1.04	108	2.0	1295	1.04
15	214	12.8	373	1.07	163	2.3	516	1.01
15 Hemisphere	142	0.01	255	1.06	138.5	5.9	59	1.03

and found to be similar to those determined from the osmium stained sample (Table 4).

For latex particles having an inverted core-shell morphology, as shown in Figs. 3A and 3B, both staining methods gave similar results due to the fact that the PS phase surrounds the major part of the PI phase. The particles behaved similarly to PS particles on analysis by TEM. Figure 3A shows latex no. 14 after OsO_4 staining, and it can be seen that the particles have a spherical shape and an inverted core-shell morphology. On staining with UAc parts of the PI phase flows out of the hollow PS particles, as shown in Fig. 3B. This behavior is consistent with an inverted core-shell morphology, where the major part of the PI forms an inclusion in the PS phase. No significant differences between the average particle diameters determined by the two staining methods were found (Table 4).

Comparison of TEM and QELS for particle size measurements

Particle size measurements carried out by TEM analysis may give erroneous results if the latex particles are partially agglomerated or if the size distribution is bimodal with one particle size being much larger than the other and present in a small number. QELS is often used for determination of particle size distributions, and gives complementary information to TEM analyses. In QELS the changes in the light intensity scattered from particles

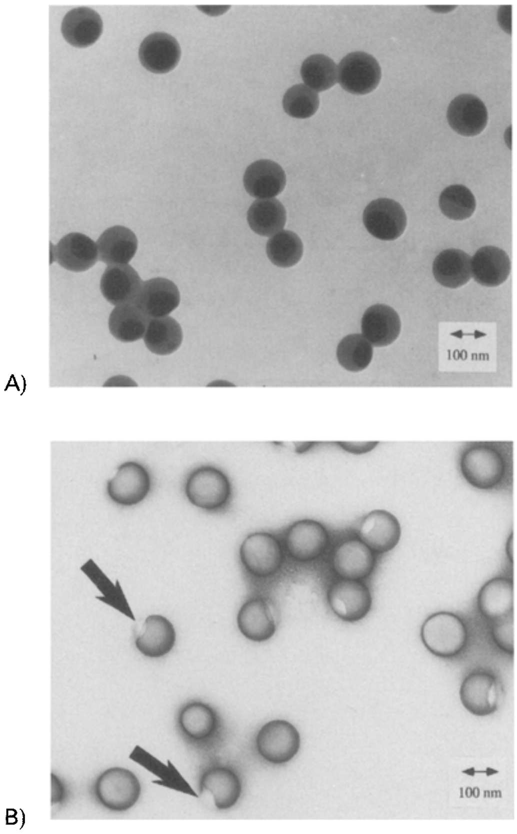

Fig. 3 TEM micrograph of latex 14. A) OsO_4 stained latex. B) UAc stained latex. PI inclusions flowing out of the PS phase are indicated by arrows

undergoing Brownian motion are measured. The intensity fluctuations are used for calculation of the average diffusion coefficient for the particles. Their average hydrodynamic diameter, d, can be calculated from the diffusion coefficient, D, by using the Stokes–Einstein equation:

$$D = \frac{kT}{3\pi\eta d}, \tag{1}$$

where k is Boltzmann's constant, T the absolute temperature, and η the viscosity of the medium. Since large particles scatter more light than small ones, large particles and agglomerates will be favored in the calculated averages. QELS is a low-resolution sizing method, and peaks in the distribution which comprise less than 10% of the total scattered intensity may be artefacts.

In order to compare results obtained from TEM and QELS, respectively, higher order averages of the distribution should be calculated from the particle sizes measured from the TEM micrographs. The light scattering average, defined as:

$$\bar{D}_{LS} = \sqrt{\frac{\sum n_i D_i^8}{\sum n_i D_i^6}} \tag{2}$$

was calculated and compared to the intensity average, $\bar{D}_I$, obtained from QELS.

In the literature various methods for determination of particle sizes and size distributions have been compared with somewhat different results [17–19]. In the present study, we measured the particle sizes using QELS, and obtained significantly larger values than by TEM measurements (Table 3d). Athey et al. [20] investigated carboxylated styrene-butadiene latexes, and they reported particle diameters measured by hydrodynamic chromatography (HDC) and disc centrifuge photosedimetry (DCP) 20–30% larger than those obtained from TEM. The larger values were explained by the immobilized water layer included in hydrodynamic diameters, or by swelling of the latex particles. Larger particle diameters were also found for charged colloidal particles [21] because of the electrical double layer. With TEM the "hard sphere cores" of the latex particles will be measured.

The relative difference, ΔD, between particle diameters measured by TEM and QELS, respectively, was in the present study calculated as $\ln(\bar{D}_I/\bar{D}_{LS})*100$. A least squares fit of ΔD as a function of the amounts of MAA and isoprene units present in the latex particles is presented as a response surface in Fig. 4. The surface represents the expected ΔD, while the numbered squares indicate the observed ΔD for each latex sample. The least squares fit was done with a 90% confidence interval for the data points. Of course, it is unlikely that a polynomial model would be a reasonable approximation of the true functional relationship over the entire space of the independent variables, but for a limited region it is usually relevant. If the fitted surface is an adequate approximation of the true response function, then an analysis of the fitted surface will be approximately equivalent to an analysis of the actual system. In Table 3e the test statistics for the difference between the observed and predicted ΔD are given. The small average $\bar{d}$ and t_0 in the statistical analysis shows that the predicted values agree well with the observed ones within the studied region. The largest uncertainty will be at the edges and in the corners of the calculated surface. With these remarks in mind some relevant, qualitative observations can be made from the plot.

All QELS measurements were made at pH 7.0 with a phosphate buffer having a ionic strength of 0.3×10^{-3} mole/L, SDS was added to a concentration of 6.9×10^{-3} mole/L, which should prevent aggregation of the latex particles. A similar comparison was made at a pH of 7.0 and a ionic strength of 6.4×10^{-7} mole/L and a sur-

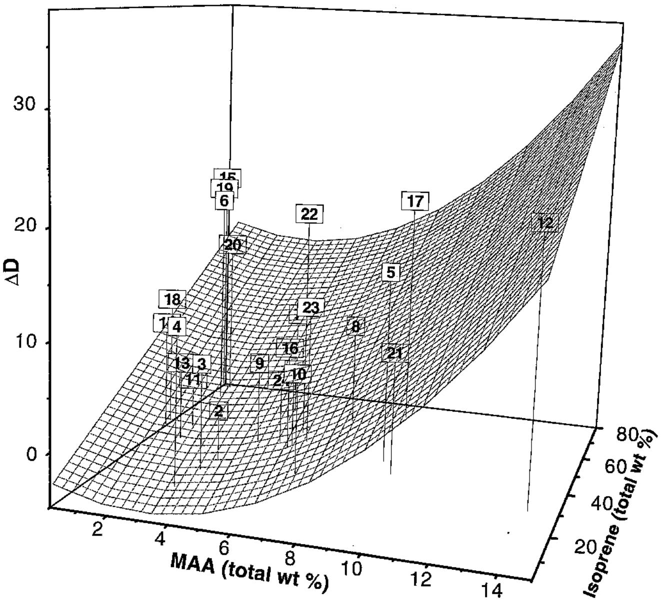

Fig. 4 Response surface plot showing the relative diameter difference, $\Delta D = \ln(\bar{D}_I/\bar{D}_{LS})*100$, as a function of the total amounts of MAA and isoprene used in the preparations of the latexes. Observed ΔD:s are presented as squares with numbers identifying each latex (see Table 2)

factant concentration on the order of 10^{-10} mole/L. At low MAA content QELS gave much larger particle diameters. The larger particle diameters found under these conditions with QELS can be explained either by partial aggregation in diluted systems [22, 23] or by a smaller diffusion coefficient due to low ionic strength [24]. In the present case the differences were negligible. The small curvature in the response surface (Fig. 4) at low MAA content is an effect of a quadric dependence of MAA in the response surface function.

At low MAA contents swelling of the particles due to water absorption should be moderate. At higher carboxylic acid contents, however, the particles swell considerably, and the diameters measured by QELS increase. The swelling of the particles will be even more accentuated at high PI contents because the particles become soft and will more easily be affected by the swelling mechanism.

The large difference in the particle diameters determined by QELS and TEM at large carboxylic acid contents, as indicated in Fig. 4, cannot be explained only by the effects of swelling. Especially in the later stages of the seeded polymerization the formation of copolymers containing large amounts of MAA may be formed. Hydrophilic loops and tails of these copolymers may be solubilized to form a hydrated corona around the particles. The corona decreases the diffusion coefficients for the particles and increases the hydrodynamic diameters recorded by QELS [25, 26]. The diameters determined by TEM will obviously not be affected. Support for this idea is given by a comparison of latex samples nos. 22 and 23. The latexes have the same overall composition, but in the preparation of no. 22 all of the MAA in step 2 was added at the end of the polymerization, while in the preparation of no. 23 the acid was added continuously during step 2. It is evident from Fig. 4 that the difference between the QELS and TEM diameters is much larger for sample no. 22 than for no. 23. The combined effects of swelling and the presence of a hydrated corona increase the hydrodynamic diameter of the particles well above the value predicted by the calculated response surface.

Conclusions

On analyzing particle sizes of film-forming heterogeneous latexes the results obtained by TEM measurements depend on the staining technique used. For styrene-isoprene latexes, OsO_4 staining gave good stability of the latex particles in the microscope, and information of the particle morphology could be obtained. UAc staining can give additional morphological information, but because the particles become deformed and form film during sample preparation the method has limited use.

Particle size measurements of film-forming, carboxylated latex particles by QELS may give too large diameters, as compared to the hard sphere particle diameters obtained by TEM. The difference in the measured diameters increases with increasing PI and PMAA content in the latex particles. The large QELS diameters may be caused by swelling, and by soluble carboxylated polymers physically adsorbed or chemically anchored to the particles, forming a hydrophilic corona.

Acknowledgements We gratefully acknowledge the financial support of this work by MoDo AB and the Swedish National Board for Industrial and Technical Development, NUTEK. We also want to thank Dr. Anders Holtsberg at the Dept. of Mathematical Statistics, Lund University, for valuable discussions and advice.

References

1. Nilsson H, Silvergren C, Törnell B (1982) Chem Scr 19:164
2. Karlsson O, Hassander H, Wesslén B, to be published
3. Kato K (1966) Polym Lett 4:35
4. Mahl H (1964) Kunstoffe 54:15
5. Davidson JA, Haller HS (1974) J Colloid Interface Sci 47:459
6. Provencher SW (1979) Makromol Chem 180:201
7. Provencher SW (1982) Comput Phys Commun 27:229

8. Cho I, Lee KW (1985) J Appl Polym Sci 30:1903
9. Lee DI, Ishikawa T (1983) J Polym Sci, Polym Chem Ed 21:147
10. Talmon Y (1987) Proc-Annu Meet, Electron Microsc Soc Am 45:496
11. Katoh M (1979) J Electron Microsc 28:197
12. Shaffer OL, El-Aasser MS, Vanderhoff JW (1987) Proc-Annu Meet, Electron Microsc Soc Am 45:502
13. Watanabe J, Seibel G, Inoue M (1984) J Polym Sci, Polym Lett. Ed 22:39
14. Brown WE (1947) J Appl Phys 18:273
15. Shaffer OL, El-Aasser MS, Vanderhoff JW (1983) Proc-Annu Meet, Electron Microsc Soc Am 41:30
16. Zosel A, Heckmann W, Ley G, Mächtle W (1987) Colloid Polym Sci 265:113
17. Klyubin VV, Kruglova LA, Sakharova NA, Tallier YuA (1990) Colloid J USSR 52:405
18. Hallett FR, Craig T, Marsh J, Nickel B (1989) Can J Spectrosc 34:63
19. Koehler ME, Provder T (1987) ACS Symp Ser 332:231
20. Athey RD, Provder T, Poehlein GW, Scolere J (1977) Colloid Polym Sci 255:1001
21. Schumacher GA, van den Ven TGM (1987) Faraday Discuss Chem Soc 83:75
22. Rowell RL, Farinato RS, Parsons JW, Ford JR, Langley KH, Stone JR, Marshall TR, Parmenter CS, Seavers M, Bradford EB (1979) J Colloid Interface Sci 69:590
23. Basset DR, Derderian EJ, Johnston JE, MacRury TB (1981) ACS Symp Ser 165:263
24. Sasaki S (1984) Colloid Polym Sci 262:406
25. Masliyah JH, Neale G, Malysa K, Van De Ven TGM (1987) Chem Eng Sci 42(2):245
26. Killmann E, Sapuntzjis P, Maier H (1992) Makromol Chem, Macromol Symp 61:42